THE JOURNAL OF PHYSICAL CHEMISTRY B

Article

pubs.acs.org/JPCB

Hydrolysis of Guanosine Triphosphate (GTP) by the Ras·GAP Protein Complex: Reaction Mechanism and Kinetic Scheme

Maria G. Khrenova,[†] Bella L. Grigorenko,[†,‡] Anatoly B. Kolomeisky,[§] and Alexander V. Nemukhin*[,†,‡]

[†]Chemistry Department, M.V. Lomonosov Moscow State University, Leninskie Gory 1/3, Moscow 119991, Russian Federation

[‡]N.M. Emanuel Institute of Biochemical Physics, Russian Academy of Sciences, Kosygina 4, Moscow 119334, Russian Federation

[§]Department of Chemistry and Center for Theoretical Biological Physics, Rice University, Houston, Texas 77005, United States

Supporting Information

ABSTRACT: Molecular mechanisms of the hydrolysis of guanosine triphosphate (GTP) to guanosine diphosphate (GDP) and inorganic phosphate (Pi) by the Ras·GAP protein complex are fully investigated by using modern modeling tools. The previously hypothesized stages of the cleavage of the phosphorus−oxygen bond in GTP and the formation of the imide form of catalytic Gln61 from Ras upon creation of Pi are confirmed by using the higher-level quantum-based calculations. The steps of the enzyme regeneration are modeled for the first time, providing a comprehensive description of the catalytic cycle. It is found that for the reaction Ras·GAP·GTP·H_2O → Ras·GAP·GDP·Pi, the highest barriers correspond to the process of regeneration of the active site but not to the process of substrate cleavage. The specific shape of the energy profile is responsible for an interesting kinetic mechanism of the GTP hydrolysis. The analysis of the process using the first-passage approach and consideration of kinetic equations suggest that the overall reaction rate is a result of the balance between relatively fast transitions and low probability of states from which these transitions are taking place. Our theoretical predictions are in excellent agreement with available experimental observations on GTP hydrolysis rates.

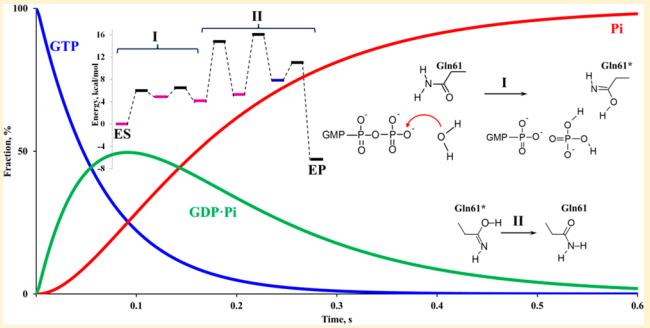

INTRODUCTION

The process of guanosine triphosphate (GTP) hydrolysis to guanosine diphosphate (GDP) and inorganic phosphate (Pi) catalyzed by the Ras protein complexed with the GTPase-activating proteins (GAPs) is crucial for many biological processes, but it is especially important for cancer research.[1,2] For this reason, it was widely investigated in recent years. The mechanism of this reaction at the atomic level has been studied employing different approaches.

Analysis of the relevant crystal structures provides some hints on how the chemical transformations can occur in this system. In this respect, the resolution of the crystal structure PDB ID 1WQ1 of Ras·GAP complexed with GDP and the γ-phosphate mimic (AlF_3) considerably contributed to clarify the subject.[3] The results of time-resolved FTIR spectroscopy provided valuable information on the molecular reaction mechanism and dynamics in the corresponding protein systems.[4−7] Other kinetic measurements on the GTP hydrolysis reaction carried on Ras molecules complexed either with p120-GAP or with another GTPase accelerating protein neurofibromin (NF1) have been also reported.[5,8−12] The basic conclusion from all these experimental studies can be formulated as follows: if the changes in GTP concentration in the chemical reactions can be measured, then the observed rate constants at temperatures near 300 K are close to 19 s^{-1}; the observed rate constants for the release of inorganic phosphate are about two times lower. However, it is not completely clear how different chemical transitions at the enzyme active site are related to each other.

From kinetic experiments, we note the paper by Phillips et al.[11] in which the individual rate constants have been determined for each stage of the GTP hydrolysis by Ras·GAP(NF1), and the measurements were performed under the same conditions such as temperature, ionic strength, etc. The major part of the kinetic scheme[11] is reproduced in eq 1.

$$\text{Ras·GTP} \overset{\text{GAP}}{\underset{1}{\rightleftharpoons}} \text{GAP·Ras·GTP} \overset{2}{\rightleftharpoons} \text{GAP·Ras·GDP·Pi} \overset{\text{Pi}}{\underset{3}{\rightleftharpoons}} \text{GAP·Ras·GDP} \overset{\text{GAP}}{\underset{4}{\rightleftharpoons}} \text{Ras·GDP} \quad (1)$$

The estimated value of the rate constant for the chemical transition **2**, which is related to the cleavage of GTP, was determined by the quenched flow method, and it was analyzed by measuring the GTP/GDP ratio by the high performance liquid chromatography. The graph in Figure 4 of ref 11 demonstrates the decay of the GTP fraction from which the rate constant can be derived, yielding k_2 = 19.5 s^{-1}. In our work, we rely on the experimental data reported for Ras·NF1[11] to justify the mechanism of GTP hydrolysis by Ras·GAP since the difference in kinetics of GTP hydrolysis in Ras accelerated either by p120-GAP or by NF1 has been shown to be small.[10]

Received: July 27, 2015
Revised: September 13, 2015
Published: September 15, 2015

DOI: 10.1021/acs.jpcb.5b07238
J. Phys. Chem. B 2015, 119, 12838−12845

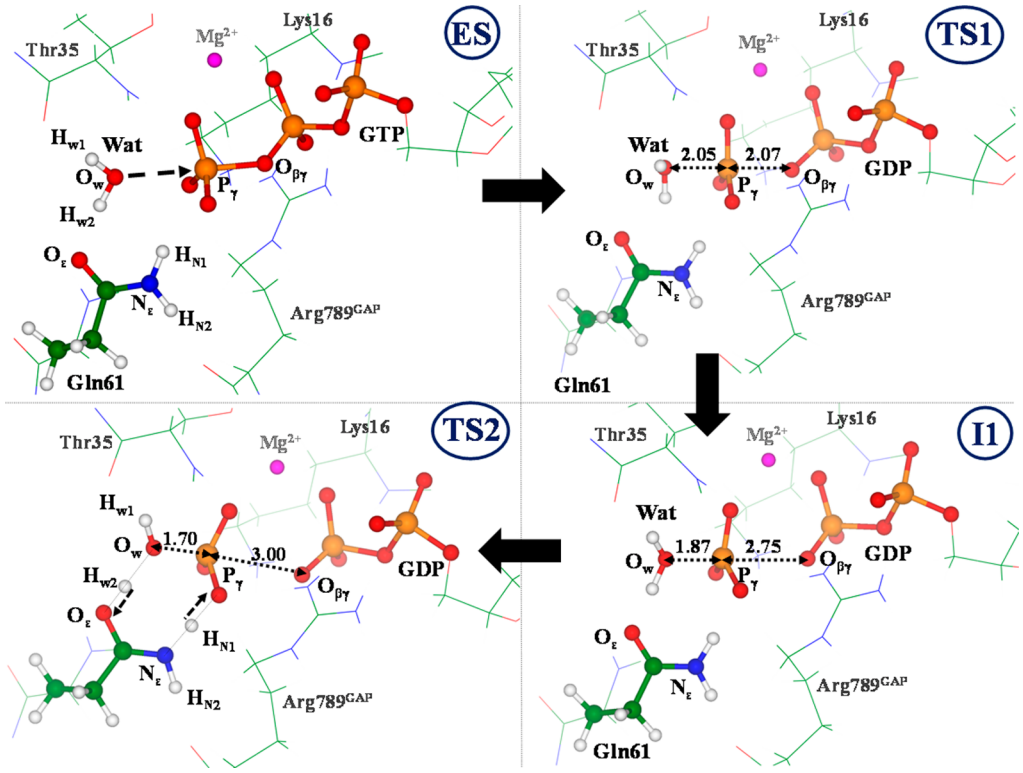

Figure 1. Chemical transformations at the active site of the Ras·GAP·GTP·H_2O complex consistent with the mechanism of the GTP hydrolysis described in refs 19 and 25−28. Here and in other figures, carbon atoms are shown in green, oxygen in red, nitrogen in blue, phosphorus in brown, hydrogen in white, and magnesium in magenta; distances are given in Å.

Computational modeling based on quantum mechanics/molecular mechanics (QM/MM) simulations[13−16] provides an important tool for understanding the reaction mechanisms in enzymes at the atomic level. Although different molecular models lead to partly overlapping conclusions when considering the GTP hydrolysis reaction[17−28] (see also the recent review articles[29−31]), there is an agreement between the results from diverse approaches.[19,25−28] According to these calculation results, the catalytic water molecule (Wat) in the enzyme−substrate complex is aligned by the hydrogen bonds with the side chains of two Ras residues, Thr35 and Gln61. The nucleophilic attack of Wat on the γ-phosphate of GTP leads to cleavage of the phosphorus−oxygen bond and separation of the $P_\gamma O_3^-$ group from GDP. Inorganic phosphate, $H_2PO_4^-$, is created following the formation of the bond between the oxygen of Wat and P_γ and proton transfer between Wat and $P_\gamma O_3^-$ through the assistance of the side chain of Gln61.

The simulations described in refs 19, 25, and 28 have been terminated at the stage when the protons are transferred and the inorganic phosphate Pi is created; however, regeneration of the active site of Ras has not been considered. To accomplish the process of enzyme regeneration, the side chain in Gln61 should be transformed from the imide to the amide form:

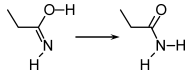

Thus, the initial motivation of the present study was to complete QM/MM simulations and to understand how the enzyme active site could be reactivated again. When the full reaction energy profile was constructed, the surprising observation was that the part referring to the process of substrate cleavage did not correspond to the highest energy barriers. Instead, the regeneration of the enzyme constituted the most energy expensive stage. Even more unexpected was the finding that such an energy diagram, showing the relatively low activation energies at the earlier chemical stages of the reaction pathway followed by higher energy barriers at the enzyme regeneration stages, was perfectly consistent with the observed kinetics of GTP hydrolysis reported by Phillips et al.[11] Correspondingly, the results of this article refer to the mechanism of chemical transformations at the active site of the Ras·GAP complex as well as to the kinetic mechanism of the GTP hydrolysis by this enzyme system.

MODELS AND METHODS

A molecular model for QM/MM calculations was constructed by using the motifs from the crystal structure PDB ID 1WQ1[3] following the protocol described in detail earlier.[27] In brief, the artificial AlF_3 group was manually replaced by the $P_\gamma O_3$ moiety; the hydrogen atoms were added assuming positive charges of the side chains Lys, Arg, and negative charges of Glu and Asp; the system was fully solvated by the shells of water molecules. The QM part comprised a large fraction of the enzyme active site: the phosphate groups of GTP, the catalytic water molecule, the side chains of Lys16, Ser17, and Gln61, the side chain and backbone of Thr35 (all from Ras), Mg^{2+} and two water molecules from the magnesium coordination shell, and the side chain of Arg789 from GAP. The quantum part included almost 90 atoms, and more than 5000 atoms in total were considered in the QM/MM scheme. For QM/MM calculations, we used the NWChem program package.[32] The QM subsystem was treated at the DFT-D3/cc-pVDZ level with the PBE0 functional[33] and the dispersion correction D3.[34] The MM subsystem was modeled with the AMBER force field

DOI: 10.1021/acs.jpcb.5b07238
J. Phys. Chem. B 2015, 119, 12838−12845

parameters.[35] Structures of the reaction intermediates were obtained in a series of unconstrained QM/MM minimizations following scans along the appropriate reaction coordinates. Vibrational analyses were performed to confirm that the located points corresponded to the true minima. Structures of the transition states (TS) separating the minimum energy areas on the energy surface were obtained as the points with single imaginary harmonic frequency. When the saddle points were located, we have verified that the descent forward and backward correctly led to the respective minimum energy structures. Finally, we introduced corrections to the potential energy values due to zero-point energies and entropic contributions.

Cartesian coordinates of atoms in the QM/MM optimized structures in the pdb format for all stationary points located in this work can be obtained from the authors upon request.

RESULTS

We summarize in Figure 1 the transformations at the initial segment of the reaction pathway of the GTP hydrolysis by Ras·GAP. The data utilized to prepare Figure 1 and also Figure 2 below were partially obtained earlier[25] and were recomputed in this work at a much higher theoretical level. The enzyme–substrate (ES) complex (the left upper panel in Figure 1) shows a proper alignment of the catalytic water molecule Wat for a nucleophilic attack on the γ-phosphate of GTP. At the first step, we gradually decreased the O_w–P_γ distance chosen as a reaction coordinate. In the first transition state, TS1 (the right upper panel in Figure 1), the $P_\gamma O_3$ group, separated from GDP, adopts a planar configuration with the almost equal distances O_w–P_γ and P_γ–$O_{\beta\gamma}$ along the in-line arrangement of the corresponding atoms. Overcoming this saddle point, the system reaches the local minimum energy point, the reaction intermediate I1 (right lower panel in Figure 1). To form the inorganic phosphate Pi with the composition $H_2PO_4^-$, the second transition state, TS2 (the left lower panel in Figure 1), should be passed to arrive to the next reaction intermediate I2 illustrated in Figure 2. The distance O_w–H_{w2} was chosen as a reaction coordinate at this step.

Specific features of the elementary step I1 → TS2 → I2 are as follows: after the formation of the covalent bond between O_w and P_γ, the protons H_{w2} (originally from Wat) and H_{N1} (originally from the amide group of Gln61) are redistributed, and the tautomer imide form of Gln61 (denoted here as Gln*61) is created.

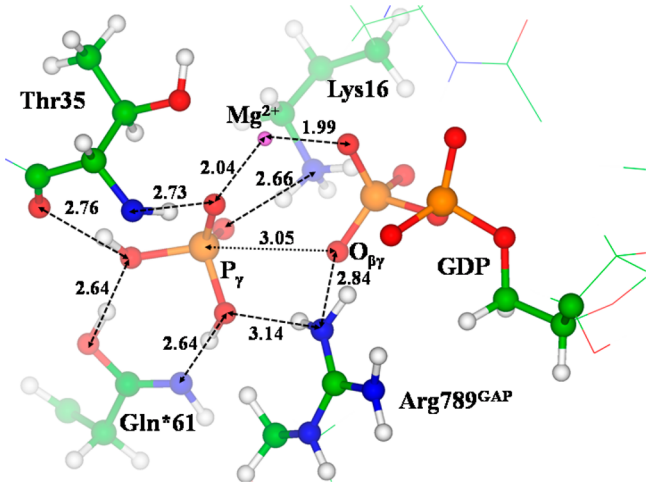

Figure 2. Fragment of the structure of the intermediate I2 obtained in the reaction pathway ES → TS1 → I1 → TS2 → I2.

Figure 2 shows that the inorganic phosphate $H_2PO_4^-$ in the I2 intermediate is conveniently located inside the protein cavity. All its oxygen atoms are saturated by hydrogen bonds, and all essential molecular groups from Ras (Thr35, Gln61, Lys16, and Mg^{2+}) and from GAP (Arg789) are involved in the binding. We discuss the energy diagrams later in the text but mention here that the QM/MM-based calculations carried out ealier[25,28] and in this work predict that the energy barriers estimated as the heights of TS1 and TS2 points above the respective minimum energy points, ES and I1, are fairly low. Importantly, the described mechanism at this segment of the reaction pathway is precisely consistent with the conclusions formulated in the recent work by Warshel et al.,[19] which followed the empirical valence bond (EVB) based simulations.

The reaction intermediate I2 corresponds to GDP and Pi trapped in the Ras*·GAP protein complex where the Ras* subunit contains the tautomer imide form of Gln61 (see Figure 2). The transformations from I2 to the enzyme–product (EP) complex, i.e., to GDP and Pi in Ras·GAP with the regenerated Gln61 side chain in the amide form are illustrated in Figure 3.

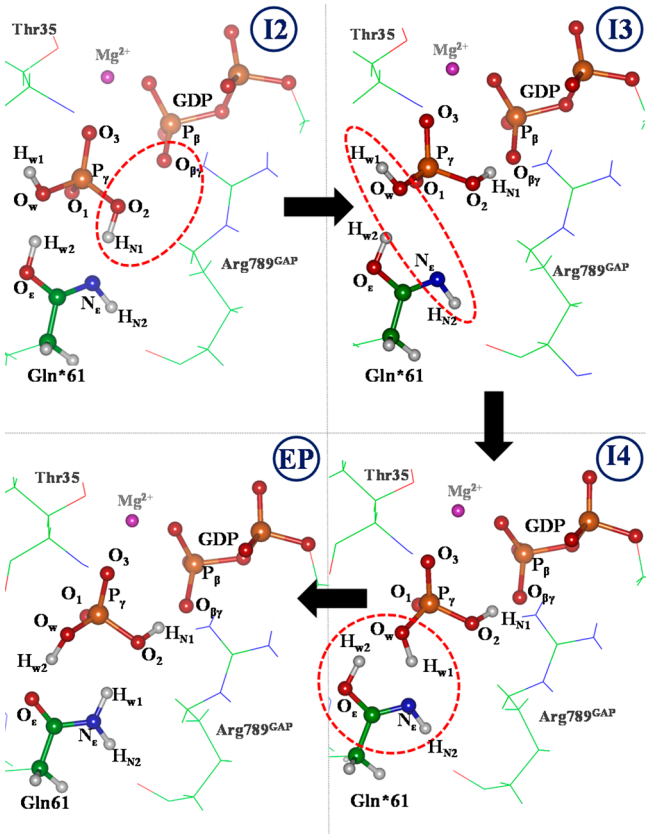

Figure 3. Transformations from I2 to EP as obtained from the QM/MM simulations.

According to our calculations, the active site regeneration of Ras starts with the rotation of the O_2–H_{N1} group around the P_γ-O_2 bond in Pi (see the left upper panel in Figure 3). As a result, the hydrogen bond between the oxygen atom $O_{\beta\gamma}$ of the β-phosphate group of GDP and H_{N1} is formed. The minimum energy structure depicted in the right upper panel in Figure 3 refers to the reaction intermediate I3. The subsequent rotation of the O_w-H_{w1} group around another phosphorus–oxygen

DOI: 10.1021/acs.jpcb.5b07238
J. Phys. Chem. B 2015, 119, 12838–12845

bond of the inorganic phosphate, P_γ-O_w, leads to the reaction intermediate I4 (the right lower panel in Figure 3). The shape of the energy surface along the I2 → TS3 → I3 and I3 → TS4 → I4 elementary steps, describing the rotations around the P-O bonds in Pi, was constructed as follows. We performed a relaxed scan along the corresponding torsion angle in order to estimate the initial coordinates of the saddle point, computed the corresponding TS geometry configuration as a point with single imaginary frequency (440i cm^{-1} for TS3 and 247i cm^{-1} for TS4), and carried out descent in forward and backward directions to connect TS with the relevant reaction intermediates.

At the final step, the protons H_{w1} and H_{w2} are redistributed between Pi and Gln61 as clarified in the left and right bottom panels in Figure 3. Like at the elementary step I1 → TS2 → I2 (Figure 1), the distance O_w–H_{w2} was chosen as a reaction coordinate at the step I4 →TS5 →EP. As a result, the amide form of Gln61 was restored. The TS5 configuration was a point on the energy surface with single imaginary frequency 1099i cm^{-1}. We present in Supporting Information the video file illustrating all transformations at the enzyme active site on the route from ES to EP.

The full energy diagram for the Ras·GAP catalyzed hydrolysis of GTP is shown in Figure 4. The calculated energy profile

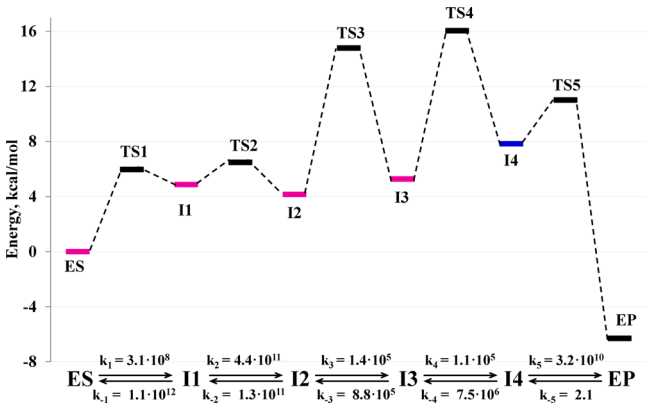

Figure 4. Energy profile for the GTP hydrolysis at the active site of the Ras·GAP complex. The bottom panel shows values of the monomolecular reaction rate constants k_{+n} and k_{-n} (in s^{-1}) estimated by using the transition state theory for every elementary step on the route.

suggests that the processes of substrate cleavage (from ES to I2) are characterized by the modest energy barriers (less than 6 kcal/mol), while the subsequent stages of enzyme regeneration (from I2 to EP) require overcoming the barriers of 10–11 kcal/mol.

We show now that such a shape of the energy landscape along the reaction coordinate is consistent with the experimental kinetic data, thus providing support to the suggested reaction mechanism. Formally, we can distinguish five elementary steps on the route from ES to EP (Figure 4) that makes stage ***2*** in the experimental kinetic scheme of eq 1. Let us consider the corresponding kinetic scheme, eq 2:

$$\mathrm{ES} \overset{1}{\rightleftarrows} \mathrm{I1} \overset{2}{\rightleftarrows} \mathrm{I2} \overset{3}{\rightleftarrows} \mathrm{I3} \overset{4}{\rightleftarrows} \mathrm{I4} \overset{5}{\rightleftarrows} \mathrm{EP} \qquad (2)$$

Application of the transition state theory to estimate the individual rate constants k_{+n} and k_{-n} (n = 1–5) for the corresponding steps leads to the values (in s^{-1}) shown in the bottom panel in Figure 4.

To prove that the computed reaction energy profile is consistent with the experimental data, we perform the following kinetics analysis. First, we used the brute-force strategy to solve numerically the set of differential equations of the kinetic scheme in eq 1 by utilizing the experimental rate constants for the stages ***1***, ***3***, and ***4*** collected in Table 3 of ref 11 and introducing our computed rate constants (see Figure 4) for stage ***2*** represented as a series of 5 elementary steps (n = 1–5). We also used in numerical calculations the experimental concentrations of enzyme and substrate.[11] Figure 5 shows the results of these simulations obtained using the computer code KINET developed for numerical modeling of the kinetic properties of complex chemical reactions.[36]

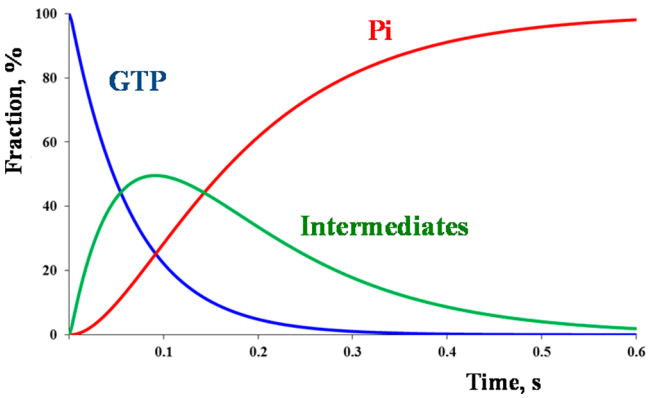

Figure 5. Computed curves for the GTP cleavage (blue) and Pi release (red). The green curve corresponds to all reaction intermediates composed of the complexes of GDP and Pi.

The computed curves for GTP and Pi reproduce remarkably well the experimental data shown in Figure 4 of ref 11. Moreover, if we fit the time dependence of GTP concentration by a single exponent function we arrive at the effective rate constant $k_{eff} \sim 15\ s^{-1}$, perfectly correlating to the measured value k_2, which is around 19 s^{-1} in all experiments at room temperature.[8,9,11,12] Ref 5 reported the results of experimental studies of GTP hydrolysis in Ras-GAP at temperature 260 K, estimating the rate constant as 0.8 s^{-1}. Our computational model applied to this temperature gives 0.15 s^{-1}.

To demonstrate the feasibility of the numerical results, we carefully analyze the kinetic scheme of eq 2 without using the experimental concentrations or experimental rate constants. We note that the energy profile shown in Figure 4 suggests that ES and the intermediates I1, I2, and I3 (the corresponding levels are marked in magenta in Figure 4) are in the pre-equilibrium state. This can be also checked by numerical solution of the kinetic differential equations: the corresponding curves for the I1, I2, and I3 concentrations decay similarly to that of ES. Thus, we can define the corresponding equilibrium constants as shown in eq 3:

$$\frac{[I_1]}{[ES]} = K_1; \quad \frac{[I_2]}{[ES]} = K_2; \quad \frac{[I_3]}{[ES]} = K_3 \qquad (3)$$

The concentration of I4 is very low, and its changes are negligible during the reaction, and this justifies the application of the steady-state approximation. The kinetic differential equations can now be written in the simpler algebraic form:

DOI: 10.1021/acs.jpcb.5b07238
J. Phys. Chem. B 2015, 119, 12838–12845

$$\frac{d[I_4]}{dt} = k_4 \cdot [I_3] - (k_5 + k_{-4}) \cdot [I_4] + k_{-5} \cdot [I_5]$$
$$\approx k_4 \cdot [I_3] - (k_5 + k_{-4}) \cdot [I_4] \approx 0 \quad (4)$$

The analytical expression for the rate of EP formation can be simplified further by ignoring the backward reaction (I4 ← EP) on the final elementary step:

$$\frac{d[I_5]}{dt} = k_5 \cdot [I_4] - k_{-5} \cdot [I_5] \approx k_5 \cdot [I_4] \quad (5)$$

Combining the above equations, we obtain the expressions for the time dependence of ES concentration:

$$-\frac{d[ES]}{dt} = \frac{d[I_5]}{dt} = \frac{K_3 \cdot k_4 \cdot k_5}{k_{-4} + k_5} \cdot [ES] \approx K_3 \cdot k_4 \cdot [ES] \quad (6)$$

Taking the values K_3 and k_4 from the data shown in the diagram in Figure 4, we get the value of effective catalytic constant as $k'_{eff} = K_3 \cdot k_{+4} \sim 17\ s^{-1}$. This is approximately the same as the one obtained from the numerical solution of the system of differential equations as discussed above.

To understand the complex kinetic mechanism of the GTP hydrolysis, it is also convenient to employ a method of first-passage processes, which is successfully utilized for analyzing multiple processes in physics, chemistry, and biology.[37] According to this approach, the overall reaction rate for multistep process eq 2 is inversely proportional to the mean first-passage time of going through the energy landscape presented in Figure 4, starting from the state ES and reaching for the first time the state EP. For sequential processes, like the hydrolysis of GTP as presented in eq 2, the explicit expressions are available.[37]

$$\tau_n = \sum_{i=1}^{n} \sum_{j=1}^{i} \frac{k_{-i+1} k_{-i+2} \times \ldots \times k_{-j}}{k_i k_{i-1} \times \ldots \times k_j} \quad (7)$$

where n is the number of sequential transitions, and the notations from those in Figure 4 are utilized. The physical meaning of this expression is clear: the average time to go from the state ES to the final state EP is a sum of residence times along the pathway. The mean first-passage time can also be viewed as an average over all trajectories that start at the initial state (ES) and finish at the final state (EP). For the hydrolysis of GTP, we have $n = 5$, and substituting the values from the calculated chemical rates yields, $\tau_5 \cong 6.75 \times 10^{-2}$ s, or $k'_{eff} \cong 15\ s^{-1}$. This result is also very close to experimentally observed kinetic measurements, supporting our theoretical arguments.

DISCUSSION

In this work, we applied the following strategy to clarify the microscopic aspects of reaction and kinetic mechanisms for the GTP hydrolysis by the Ras·GAP protein complex. First, we computed the energy profile connecting the reactants and products trapped inside the enzyme and specified all elementary steps along the pathway. Analysis of the located structures of the minimum energy points and of the saddle points characterized the qualitative sides of the reaction mechanism. An essential part of this mechanism is a temporary formation of the reaction intermediate with the tautomerized form of Gln61 from Ras. Regeneration of the enzyme active site required transformation of this form to the amide isomer. Second, the QM/MM simulations allowed us to estimate the energy diagrams at each step and to obtain the corresponding barriers for forward and backward reactions. These barriers were corrected by adding the zero-point energies and entropic contributions, and such obtained values were converted to the monomolecular reaction rate constants k_{+n} and k_{-n} by using the transition state theory for every elementary step on the route. Then, we applied three approaches to evaluate the effective rate constant k_{eff} for this multistep process: (i) the brute-force numerical solution of the set of differential equations describing the full kinetic scheme by utilizing the experimental[11] rate constants for the stages *1*, *3*, and *4* identified in eq 1 and introducing our computed rate constants for the stage *2* represented as a series of 5 elementary steps; (ii) analytical solution of the appropriate kinetic eqs eq 2−6; and (iii) estimation by the method of first-passage processes, eq 7. All approaches resulted in consistent values of constant k_{eff}, which remarkably well correlated with the measured rate constants of the GTP hydrolysis in this protein system.

From the qualitative side, the kinetics of the fairly slow decay of GTP despite the very low activation barriers on the part of the energy profile responsible for GTP cleavage (from ES to I2) is understandable because multiple forward and backward transitions between the substrate and the reaction intermediates I1, I2, and I3 occur before the reactants finally overcome TS4 and TS5. We also point out that the importance of the first-passage method is that it allows us to explain better the molecular picture of this process. Using the calculated values from Figure 4, it can be shown that the mean first-passage time is dominated by just two terms:

$$\tau_5 \cong \frac{1}{K_2 k_3} + \frac{1}{K_3 k_4} = (0.75 + 6.00) \times 10^{-2} s \quad (8)$$

This suggests that in the hydrolysis cycle, the system spends most of the time in states I2 and I3. The rate limiting steps are passing the barriers TS3 and TS4, but the overall rate is much smaller than these specific rates (k_3 and k_4) because the fraction of molecules in states I2 and I3 is relatively small. Fast reactions of GTP cleavage (first two barriers) quickly lead to effective pre-equilibrium conditions, and energetically, states I2 and I3 are higher in energy than the original ES state. As a result, the fraction of molecule in states I2 and I3 is significantly smaller than that in state ES. The flux over the barrier is a product of the concentration of molecules in the state preceding the barrier times the rate of passing the barrier. Thus, the overall kinetic rate here is a balance between relatively fast transitions and a low probability of states from which these transitions are taking place.

The reaction mechanism and the kinetic scheme considered in this work rely on the assumption that there is only one water molecule at the active site of the Ras·GTP·GAP complex. If the protein cavity was less tight and at least two water molecules could be incorporated near the γ-phosphate group of GTP, then different scenarios might be considered. One of the possible options might be a mechanism that does not involve the temporary formation of the tautomer form of Gln61. We computationally characterized such a reaction pathway earlier[26] for the case of GTP hydrolysis by Ras without GAP. It was shown, in particular, that the computed barriers on the pathway Ras(Gln61)·GTP·H_2O·H_2O → Ras(Gln61)·GDP·Pi·H_2O were considerably higher than that in the reaction Ras(Gln61)·GAP·GTP·H_2O → Ras(Gln*61)·GAP·GDP·Pi. If two water molecules could still be found at the active site and the imide form of Gln61 was assumed to be on the reaction pathway upon the formation of Pi, then, of course, the tautomeric Gln*

DOI: 10.1021/acs.jpcb.5b07238
J. Phys. Chem. B 2015, 119, 12838−12845

→ Gln transformation would be considerably facilitated by the second water molecule.

However, we do not find clear evidence for the presence of two (or more) water molecules at the active site in the Ras·GTP·GAP structure. A study of Martín-García et al.,[23] which reports the results of QM(PM3)/MM calculations on the mechanism of GTP hydrolysis by Ras-GAP, is sometimes invoked as an argument that supports such a hypothesis. As a motivation of their work, the authors of ref 23 claimed that the involvement of the second water molecule in the catalytic mechanism was suggested by the cryo-technique studies by Scheidig, Burmester, and Goody et al.[38] However, this is not a correct reference since in the latter work the GTP hydrolysis in Ras but not in Ras-GAP has been experimentally studied.[39] The conclusions from the computations,[23] suggesting that two water molecules operate in the cavity of the Ras·GTP·GAP complex, also might not be reliable because of the application of the semiempirical PM3 Hamiltonian in the QM part. Shortcomings of the PM3 methodology in describing hydrogen bonds, which is crucial for modeling protein systems, are well-known; see, e.g., ref 39. For these reasons, more advanced procedures have been introduced in recent years.[40,41] Most likely, the protein structures obtained in ref 23 in the molecular dynamics simulations with the QM(PM3)/MM potentials are not correct. On the contrary, all our QM/MM simulations[25−28] using *ab initio* quantum chemistry methods show a good agreement with the crystal structure PDB ID 1WQ1,[3] supporting our arguments. This also indicates that there is no need to introduce more than one water molecule at the active site. However, some recent evidence shows that there is a possibility of the presence of a second water molecule near the vicinity of the active site and that the resulting path should have a low barrier. Hence, computationally it is advantageous to explore all possible mechanistic pathways explicitly rather than assuming them.

Returning to the mechanism of GTP hydrolysis by Ras-GAP described in this work as well as in our previous papers,[25−28] we should comment that the step I1 → I2 suggesting the concerted proton transfers and the formation of the tautomer imide form of Gln61 seems to be unexpected at first glance, although such a scenario has been suspected in a crystallography study of Sondek et al.[13] by analyzing the hydrolysis of GTP by another GTPase, transducin alpha.[42] In fact, we performed countless, but unsuccessful attempts by exploring QM/MM-based simulations to find a pathway that would allow one to avoid a consideration of the tautomer form of Gln61. Of course, we cannot exclude the fact that sampling based QM/MM computations will be helpful to find alternative reaction routes. In the most recent works,[27,28] we computed the free energy profiles for the process ES → I2 by using MD simulations with the QM/MM potentials. The results of MD calculations provided clear visualization of the molecular events along trajectories. Accordingly, we could observe proton transfers corresponding to the step I1 → I2 with the formation of Gln*61 when applying steered MD along the O_w−Pγ coordinate.

Consideration of the proton movement from Wat to the carbonyl oxygen of Gln61 followed by intramolecular proton transfer presents one more possible scenario. We did not obtain the corresponding reaction intermediates in the Ras-GAP catalyzed GTP hydrolysis; however, we could locate such an intermediate in the simulations of GTP hydrolysis by another GTPase, Arl3, complexed with its GAP, RP2.[43] Even in this case, the next step from this intermediate with the protonated carbonyl oxygen of Gln again resulted in the tautomer imide form of glutamine.

Therefore, most probably, the role of Gln61 in the Ras-GAP catalyzed hydrolysis of GTP is to take part in the proton transfer steps. This conclusion does not contradict the results described in the works of Warshel et al.[18,19] In fact, the EVB based simulations illustrated in Figure 3 of ref 19 demonstrate similar proton transfer events as shown in Figure 1 and Figure 2 of the present article. An elegant analysis of the electrostatic contributions of the protein amino acid residues going from the ES state to the state corresponding to our intermediate I2 performed in ref 19 shows different contributions for the P-loop, switch I, switch II, and Mg^{2+} ion region, which is consistent with the allosteric effects associated, in particular, with Gln61.

We should also comment on the role of Gln61 in the Ras-GAP catalyzed hydrolysis of GTP from the point of view of the mutational studies. One of the key experiments with the Gln61 mutation was reported by Schultz et al.[44] who found that a substitution of the Gln61 residue with an unnatural amino acid NGln, an isoelectronic, isosteric nitro analogue of Gln, had little effect on the hydrolysis rate. By using QM/MM simulations similar to those described in the present work, we could demonstrate that both glutamine and its nitro analogue in the *aci*-nitro form participated in the reaction of GTP hydrolysis at the stages of proton transfer and formation of inorganic phosphate. The computed structures and the energy profiles for the complete pathway from the enzyme−substrate to enzyme−product complexes for the wild-type and mutated Ras suggest that the reaction mechanism is not affected by this mutation.[45]

Finally, we comment on the kinetic scheme consistent with the energy profile depicted in Figure 4. It should be noted that the dominant dynamic behavior is determined by the difference between the largest barrier (here, TS4) and the lowest state (ES) in the pathway. Using the transition state theory formulas for room temperature, this difference, 16 kcal/mol, can be converted to the reaction rate constant 19 s^{-1} in precise agreement with the experimental data. However, we believe that consideration of all kinetic equations provides more important information on mechanisms in this process. In particular, it predicts in what intermediate states the system spends most of the time, I2 and I3 for our system, which is consistent with the experimental data presented in Figure 4 of ref 11. This approach allows us to explicitly evaluate the contributions from transitions with similar rates, which might be important for the systems with comparable barriers, as found in our case.

Our theoretical analysis raises an interesting fundamental question on why the GTP hydrolysis follows this kinetic scheme. We suggest that this might be due to the fact that several earlier chemical steps related to the substrate cleavage control this reaction. It is much easier from an energetic point of view to modify some of these steps instead of trying to change the regeneration of enzymes.

■ CONCLUSIONS

There are two important results from our theoretical analysis. First, the full reaction mechanism of the GTP hydrolysis by Ras·GAP, which is one of the most important biochemical reactions, has been proposed and quantified. Second, we are able to provide a microscopic explanation of the kinetic scheme for the GTP hydrolysis. Consistent with experimental data, the

DOI: 10.1021/acs.jpcb.5b07238
J. Phys. Chem. B 2015, 119, 12838−12845

decay of the substrate concentration upon hydrolysis is explained by the processes that involve enzyme regeneration and not only by the stage of chemical cleavage of the substrate.

■ ASSOCIATED CONTENT

Supporting Information

The Supporting Information is available free of charge on the ACS Publications website at DOI: 10.1021/acs.jpcb.5b07238.

Video file demonstrating chemical transformations at the active site of Ras-GAP in GTP hydrolysis (MPG)

■ AUTHOR INFORMATION

Corresponding Author

*Phone: +7-495-939-10-96. E-mail: anemukhin@yahoo.com; anem@lcc.chem.msu.ru.

Notes

The authors declare no competing financial interest.

■ ACKNOWLEDGMENTS

We thank Professor B.V. Romanovsky and Professor S.D. Varfolomeev for valuable advice and E.D. Kots for help in preparing the video materials. This study was partially supported by the Russian Foundation for Basic Researches (15-33-20579). We acknowledge the use of supercomputer resources of the M.V. Lomonosov Moscow State University[46] and of the Joint Supercomputer Center of the Russian Academy of Sciences. A.B.K. acknowledges the support from the Welch Foundation (Grant C-1559), from the NSF (Grant CHE-1360979), and from the Center for Theoretical Biological Physics sponsored by the NSF (Grant PHY-1427654).

■ REFERENCES

(1) Cox, A. D.; Der, C. J. Ras History: The Saga Continues. *Small GTPases* **2010**, *1*, 2−27.

(2) Malumbres, M.; Barbacid, M. RAS Oncogenes: The First 30 Years. *Nat. Rev. Cancer* **2003**, *3*, 459−465.

(3) Scheffzek, K.; Ahmadian, M. R.; Kabsch, W.; Wiesmuller, L.; Lautwein, A.; Schmitz, F.; Wittinghofer, A. The Ras-RasGAP Complex: Structural Basis for GTPase Activation and its Loss in Oncogenic Ras Mutants. *Science* **1997**, *277*, 333−338.

(4) Kötting, C.; Blessenohl, M.; Suveyzdis, Y.; Goody, R. S.; Wittinghofer, A.; Gerwert, K. A Phosphoryl Transfer Intermediate in the GTPase Reaction of Ras in Complex with its GTPase-Activating Protein. *Proc. Natl. Acad. Sci. U. S. A.* **2006**, *103*, 13911−13916.

(5) Kötting, C.; Kallenbach, A.; Suveyzdis, Y.; Wittinghofer, A.; Gerwert, K. The GAP Arginine Finger Movement into the Catalytic Site of Ras Increases the Activation Entropy. *Proc. Natl. Acad. Sci. U. S. A.* **2008**, *105*, 6260−6265.

(6) Rudack, T.; Xia, F.; Schlitter, J.; Kötting, C.; Gerwert, K. Ras and GTPase-Activating Protein (GAP) Drive GTP into a Precatalytic State as Revealed by Combining FTIR and Biomolecular Simulations. *Proc. Natl. Acad. Sci. U. S. A.* **2012**, *109*, 15295−15300.

(7) Xia, F.; Rudack, T.; Cui, Q.; Kötting, C.; Gerwert, K. Detailed Structure of the $H_2PO_4^{(-)}$-Guanosine Diphosphate Intermediate in Ras-GAP Decoded from FTIR Experiments by Biomolecular Simulations. *J. Am. Chem. Soc.* **2012**, *134*, 20041−20044.

(8) Gideon, P.; John, J.; Frech, M.; Lautwein, A.; Clark, R.; Scheffler, J. E.; Wittinghofer, A. Mutational and Kinetic Analyses of the GTPase-Activating Protein (GAP)-p21 Interaction: The C-Terminal Domain of GAP is not Sufficient for Full Activity. *Mol. Cell. Biol.* **1992**, *12*, 2050−2056.

(9) Schweins, T.; Geyer, M.; Scheffzek, K.; Warshel, A.; Kalbitzer, H. R.; Wittinghofer, A. Substrate-Assisted Catalysis as a Mechanism for GTP Hydrolysis of p21ras and other GTP-Binding Proteins. *Nat. Struct. Biol.* **1995**, *2*, 36−44.

(10) Nixon, A. E.; Brune, M.; Lowe, P. N.; Webb, M. R. Kinetics of Inorganic Phosphate Release during the Interaction of p21ras with the GTPases-Activating Proteins, p120-GAP and Neurofibromin. *Biochemistry* **1995**, *34*, 15592−15598.

(11) Phillips, R. A.; Hunter, J. L.; Eccleston, J. F.; Webb, M. R. The Mechanism of Ras GTPase Activation by Neurofibromin. *Biochemistry* **2003**, *42*, 3956−3965.

(12) Wey, M.; Lee, J.; Jeong, S. S.; Kim, J.; Heo, J. Kinetic Mechanisms of Mutation-Dependent Harvey Ras Activation and their Relevance for the Development of Costello Syndrome. *Biochemistry* **2013**, *52*, 8465−8479.

(13) Warshel, A.; Levitt, M. Theoretical Studies of Enzymic Reactions: Dielectric Electrostatic and Steric Stabilization of the Carbonium Ion in the Reaction of Lysozyme. *J. Mol. Biol.* **1976**, *103*, 227−249.

(14) Senn, H. M.; Thiel, W. QM/MM Methods for Biomolecular Systems. *Angew. Chem., Int. Ed.* **2009**, *48*, 1198−229.

(15) Merz, K. M., Jr. Using Quantum Mechanical Approaches to Study Biological Systems. *Acc. Chem. Res.* **2014**, *47*, 2804−2811.

(16) van der Kamp, M. V.; Mulholland, A. J. Combined Quantum Mechanics/Molecular Mechanics (QM/MM) Methods in Computational Enzymology. *Biochemistry* **2013**, *52*, 2708−2728.

(17) Glennon, T. M.; Villa, J.; Warshel, A. How Does GAP Catalyze the GTP Reaction of Ras? A Computer Simulation Study. *Biochemistry* **2000**, *39*, 9641−9651.

(18) Shurki, A.; Warshel, A. Why Does the Ras Switch "Break" by Oncogenic Mutations? *Proteins: Struct., Funct., Genet.* **2004**, *55*, 1−10.

(19) Prasad, B. R.; Plotnikov, N. V.; Lameira, J.; Warshel, A. Quantitative Exploration of the Molecular Origin of the Activation of GTPase. *Proc. Natl. Acad. Sci. U.S.A.* **2013**, *110*, 20509−20514.

(20) te Heesen, H.; Gerwert, K.; Schlitter, J. Role of the Arginine Finger in Ras.RasGAP Revealed by QM/MM Calculations. *FEBS Lett.* **2007**, *581*, 5677−5684.

(21) Xia, F.; Rudack, T.; Kötting, C.; Schlitter, J.; Gerwert, K. The Specific Vibrational Modes of GTP in Solution and Bound to Ras: A Detailed Theoretical Analysis by QM/MM Simulations. *Phys. Chem. Chem. Phys.* **2011**, *13*, 21451−21460.

(22) Rudack, T.; Xia, F.; Schlitter, J.; Kötting, C.; Gerwert, K. The role of magnesium for Geometry and Charge in GTP Hydrolysis, Revealed by Quantum Mechanics/Molecular Mechanics Simulations. *Biophys. J.* **2012**, *103*, 293−302.

(23) Martín-García, F.; Mendieta-Moreno, J. I.; López-Viñas, E.; Gómez-Puertas, P.; Mendieta, J. The Role of Gln61 in HRas GTP Hydrolysis: A Quantum Mechanics/Molecular Mechanics Study. *Biophys. J.* **2012**, *102*, 152−157.

(24) Topol, I. A.; Cachau, R. E.; Nemukhin, A. V.; Grigorenko, B. L.; Burt, S. K. Quantum Chemical Modeling of the GTP Hydrolysis by the RAS-GAP Protein Complex. *Biochim. Biophys. Acta, Proteins Proteomics* **2004**, *1700*, 125−36.

(25) Grigorenko, B. L.; Nemukhin, A. V.; Topol, I. A.; Cachau, R. E.; Burt, S. K. QM/MM Modeling the Ras−GAP Catalyzed Hydrolysis of Guanosine Triphosphate. *Proteins: Struct., Funct., Genet.* **2005**, *60*, 495−503.

(26) Grigorenko, B. L.; Nemukhin, A. V.; Shadrina, M. S.; Topol, I. A.; Burt, S. K. Mechanisms of Guanosine Triphosphate Hydrolysis by Ras and Ras-GAP Proteins as Rationalized by Ab Initio QM/MM Simulations. *Proteins: Struct., Funct., Genet.* **2007**, *66*, 456−466.

(27) Khrenova, M. G.; Mironov, V. A.; Grigorenko, B. L.; Nemukhin, A. V. Modeling the Role of G12V and G13V Ras Mutations in the RasGAP Catalyzed Hydrolysis Reaction of Guanosine Triphosphate. *Biochemistry* **2014**, *53*, 7093−7099.

(28) Mironov, V. A.; Khrenova, M. G.; Lychko, L. A.; Nemukhin, A. V. Computational Characterization of the Chemical Step in the GTP Hydrolysis by Ras-GAP for the Wild-Type and G13V Mutated Ras. *Proteins: Struct., Funct., Genet.* **2015**, *83*, 1046−1053.

(29) Prakash, P.; Gorfe, A. A. Overview of Simulation Studies on the Enzymatic Activity and Conformational Dynamics of the GTPase Ras. *Mol. Simul.* **2014**, *40*, 839−847.

DOI: 10.1021/acs.jpcb.5b07238
J. Phys. Chem. B 2015, 119, 12838−12845

(30) Carvalho, A. T. P.; Szeler, K.; Vavitsas, K.; Åqvist, J.; Kamerlin, S. C. L. Modeling the Mechanisms of Biological GTP Hydrolysis. *Arch. Biochem. Biophys.* **2015**, *582*, 80−90.
(31) Kötting, C.; Gerwert, K. What Vibrations Tell Us about GTPases. *Biol. Chem.* **2015**, *396*, 131−144.
(32) Valiev, M.; Bylaska, E. J.; Govind, N.; Kowalski, K.; Straatsma, T. P.; van Dam, H. J. J.; Wang, D.; Nieplocha, J.; Apra, E.; Windus, T. L.; et al. NWChem: A Comprehensive and Scalable Open-Source Solution for Large Scale Molecular Simulations. *Comput. Phys. Commun.* **2010**, *181*, 1477−1489.
(33) Adamo, C.; Barone, V. Toward Reliable Density Functionals without Adjustable Parameters: The PBE0Model. *J. Chem. Phys.* **1999**, *110*, 6158−6170.
(34) Grimme, S.; Antony, J.; Ehrlich, S.; Krieg, H. A Consistent and Accurate Ab Initio Parameterization of Density Functional Dispersion Correction (DFT-D) for the 94 Elements H-Pu. *J. Chem. Phys.* **2010**, *132*, 154104.
(35) Cornell, W. D.; Cieplak, P.; Bayly, C. I.; Gould, I. R.; Merz, K. M.; Ferguson, D. M.; Spellmeyer, D. C.; Fox, T.; Caldwell, J. W.; Kollman, P. A. A Second Generation Force Field for the Simulation of Proteins, Nucleic Acids, and Organic Molecules. *J. Am. Chem. Soc.* **1995**, *117*, 5179−5197.
(36) Abramenkov, A. V. KINET, Software for Numerical Modeling Kinetics of Complex Chemical Reactions. www.chem.msu.su/rus/teaching/KINET2012 (Accessed on Jul 17, 2015).
(37) Van Kampen, N. G. *Stochastic Processes in Physics and Chemistry*, 3rd ed.; North-Holland Personal Library: Amsterdam, 2007.
(38) Scheidig, A. J.; Burmester, C.; Goody, R. S. The Pre-Hydrolysis State of p21(Ras) in Complex with GTP: New Insights into the Role of Water Molecules in the GTP Hydrolysis Reaction of Ras-like Proteins. *Structure* **1999**, *7*, 1311−1324.
(39) Gleeson, M. P.; Gleeson, D. QM/MM Calculations in Drug Discovery: A Useful Method for Studying Binding Phenomena? *J. Chem. Inf. Model.* **2009**, *49*, 670−677.
(40) Stewart, J. J. Application of the PM6Method to Modeling Proteins. *J. Mol. Model.* **2009**, *15*, 765−808.
(41) Yilmazer, N. D.; Korth, M. Enhanced Semiempirical QM Methods for Biomolecular Interactions. *Comput. Struct. Biotechnol. J.* **2015**, *13*, 169−175.
(42) Sondek, J.; Lambright, D. G.; Noel, J. P.; Hamm, H. E.; Sigler, P. B. GTPase Mechanism of G Proteins from the 1.7-A Crystal Structure of Transducin Alpha-GDP-AIF-4. *Nature* **1994**, *372*, 276−279.
(43) Veltel, S.; Gasper, R.; Eisenacher, E.; Wittinghofer, A. The Retinitis Pigmentosa 2 Gene Product Is a GTPase Activating Protein for Arf-like 3. *Nat. Struct. Mol. Biol.* **2008**, *15*, 373−380.
(44) Chung, H.-H.; Benson, D. R.; Schultz, P. G. Probing the Structure and Mechanism of Ras Protein with an Expanded Genetic Code. *Science* **1993**, *259*, 806−809.
(45) Khrenova, M. G.; Grigorenko, B. L.; Mironov, V. A.; Nemukhin, A. V. Why Does Mutation of Gln61 in Ras by the Nitro Analog NGln Maintain Activity of Ras-GAP in Hydrolysis of Guanosine Triphosphate? *Proteins: Struct., Funct., Genet.*, in press. DOI: 10.1002/prot.24927
(46) Voevodin, Vl.V.; Zhumatiy, S. A.; Sobolev, S. I.; Antonov, A. S.; Bryzgalov, P. A.; Nikitenko, D. A.; Stefanov, K. S.; Voevodin; Vad, V. Practice of "Lomonosov" Supercomputer. *Open Systems J. (Mosc.)* **2012**, *7*, 36−39.

DOI: 10.1021/acs.jpcb.5b07238
J. Phys. Chem. B 2015, 119, 12838−12845